Biomaterials 33 (2012) 4555–4564

Contents lists available at SciVerse ScienceDirect

Biomaterials

journal homepage: www.elsevier.com/locate/biomaterials

The effects of intrathecal injection of a hyaluronan-based hydrogel on inflammation, scarring and neurobehavioural outcomes in a rat model of severe spinal cord injury associated with arachnoiditis

James W. Austin [a,d,1], Catherine E. Kang [c,e,2], M. Douglas Baumann [c,e,2], Lisa DiDiodato [f,3], Kajana Satkunendrarajah [d,1], Jefferson R. Wilson [b,4], Greg J. Stanisz [f,5], Molly S. Shoichet [c,e,6], Michael G. Fehlings [a,b,d,*]

[a] Institute of Medical Science, University of Toronto, Canada
[b] Department of Surgery, Division of Neurosurgery, University of Toronto, Canada
[c] Department of Chemical Engineering & Applied Chemistry, University of Toronto, Canada
[d] Division of Genetics and Development and Krembil Neuroscience Centre, Toronto Western Research Institute, University Health Network, Toronto, Canada
[e] Institute of Biomaterials and Biomedical Engineering, Toronto, Canada
[f] Sunnybrook Health Sciences Center, Toronto, Canada

ARTICLE INFO

Article history:
Received 2 February 2012
Accepted 6 March 2012
Available online 27 March 2012

Keywords:
Hyaluronan
Inflammation
Fibrosis
Spinal cord injury
Hydrogel

ABSTRACT

Traumatic spinal cord injury (SCI) comprises a heterogeneous condition caused by a complex array of mechanical forces that damage the spinal cord – making each case somewhat unique. In addition to parenchymal injury, a subset of patients experience severe inflammation in the subarachnoid space or arachnoiditis, which can lead to the development of fluid-filled cavities/syringes, a condition called post-traumatic syringomyelia (PTS). Currently, there are no therapeutic means to address this devastating complication in patients and furthermore once PTS is diagnosed, treatment is often prone to failure. We hypothesized that reducing subarachnoid inflammation using a novel bioengineered strategy would improve outcome in a rodent model of PTS. A hydrogel of hyaluronan and methyl cellulose (HAMC) was injected into the subarachnoid space 24 h post PTS injury in rats. Intrathecal injection of HAMC reduced the extent of fibrosis and inflammation in the subarachnoid space. Furthermore, HAMC promoted improved neurobehavioural recovery, enhanced axonal conduction and reduced the extent of the lesion as assessed by MRI and histomorphometric assessment. These findings were additionally associated with a reduction in the post-traumatic parenchymal fibrous scar formation as evidenced by reduced CSPG deposition and reduced IL-1α cytokine levels. Our data suggest that HAMC is capable of modulating inflammation and scarring events, leading to improved functional recovery following severe SCI associated with arachnoiditis.

1. Introduction

Traumatic spinal cord injury (SCI) causes motor, sensory and autonomic impairments that lead to considerable patient suffering and which have substantial economic implications. Currently, there are few effective pharmacological treatment options to complement surgical and rehabilitation measures undertaken by physicians and health care practitioners. Damage to meningeal layers is an often overlooked aspect of the primary trauma following SCI. Acute arachnoiditis can not only potentiate parenchymal inflammation and scarring but also lead to the formation of chronic subarachnoid scarring or adhesions, a phenomenon associated with the development of parenchymal fluid-filled cavities – or what is known as post-traumatic syringomyelia (PTS) [1]. It has

* Corresponding author. Genetics and Development, Toronto Western Research Institute , 399 Bathurst St., McL 12-407, Toronto, ON, Canada M5T 2S8. Tel.: +1 416 603 5627; fax: +1 416 603 5298.
E-mail address: michael.fehlings@uhn.on.ca (M.G. Fehlings).
[1] Toronto Western Hospital, 399 Bathurst St. McL 12-407, Toronto, ON, Canada M5T 2S8.
[2] Terrence Donnelly Centre for Cellular & Biomolecular Research 160 College Street, Room 530, Toronto, ON, Canada M5S 3E1.
[3] Toronto Medical Discovery Tower 101 College St 7-206, Toronto, ON, Canada M5G 1L7.
[4] University of Toronto, Division of Neurosurgery Toronto Western Hospital 399 Bathurst St. Toronto, ON, Canada M5T 2S8.
[5] Sunnybrook Health Sciences Centre 2075 Bayview Ave., Rm S656, Toronto, ON, Canada M4N 3M5.
[6] Terrence Donnelly Centre for Cellular & Biomolecular Research 160 College Street, Room 514 Toronto, ON, Canada M5S 3E1.

0142-9612/$ – see front matter © 2012 Elsevier Ltd. All rights reserved.
doi:10.1016/j.biomaterials.2012.03.022

been estimated that up to 5% of injuries will develop symptomatic PTS from weeks to years following injury [2–6]. Syrinx development is thought to occur due to subarachnoid scarring mediated alterations in CSF flow dynamics, resulting in increased inflow of CSF [1,7–9]. Importantly, PTS represents a complication of SCI that is responsible for increased neuropathic pain and decreased motor function [10,11].

Our PTS model consistently produces the clinical features of PTS [12]. Although arachnoiditis is artificially induced in this model, the kaolin injection produces more severe arachnoiditis/scarring that is seen clinically in PTS patients and also increases parenchymal inflammation, gliosis and decreases functional recovery relative to SCI alone [12]. This suggests that targeting early arachnoiditis could have a significant impact on SCI pathology during this time period and improve long-term functional recovery. Currently, there are no preventive treatment options to reduce subarachnoid scarring. Further, the likelihood of recurrence following surgical intervention for PTS (arachnolysis/detethering) can be as high as 83% in cases of extensive scarring [1].

Hydrogels comprised of fibrin [13], polyethylene glycol [14,15], chitosan [16], 2-hydroxyethyl methacrylate [17] and hyaluronan-based biomaterials [18] have been studied in a variety of spinal cord injury repair strategies. Hyaluronan (HA) is particularly compelling, as high molecular weight HA plays a role in inflammation and tissue repair by interacting with inflammatory cells and ECM proteins (see [19] for a review). When a physical blend of hyaluronan and methyl cellulose (MC), HAMC, was injected in the intrathecal space (the fluid-filled cavity that surrounds the spinal cord) it attenuated the inflammatory response after spinal cord injury [20], and degraded/dissolved after 4–7 days therein [21]. We hypothesized that intrathecal injection of HAMC [20] would reduce arachnoiditis and improve functional recovery in our rat model of PTS [12]. In the present paper, to test this hypothesis, HAMC was injected into the intrathecal space 24 h after severe SCI and PTS was induced in a rat animal model. Tissue was characterized in terms of arachnoiditis and subarachnoid scarring, lesion size and extent of fibrous scar formation relative to artificial cerebrospinal fluid (aCSF) controls. The rats were further characterized for functional repair in terms of neurobehavioural recovery and axonal conduction relative to controls. To gain greater insight into the mechanism of repair, cytokine expression and axonal preservation were compared in HAMC treated animals versus controls.

2. Methods

2.1. HAMC preparation

HA (1,700,000 Da) was purchased from Lifecore (Chaska, MN, USA) and MC (13,000 Da) was purchased from Sigma Aldrich (St Louis, MO, USA). HA was sterilized by filtering a 0.1% solution through a 0.2 μm filter and lyophilizing prior to use. MC was sterilized similarly. Following lyophilization, sterile HAMC was produced by mixing polymer solutions in a laminar flow hood. aCSF was prepared in dH_2O with 148 mM NaCl, 3 mM KCl, 0.8 mM $MgCl_2$, 1.4 mM $CaCl_2$, 1.5 mM Na_2HPO_4, and 0.2 mM NaH_2PO_4. The MC and HA powders were sequentially dissolved in aCSF at 4 °C, resulting in a 2% HA and 7% MC solution.

2.2. PTS model

All animal protocols were approved by the animal ethics board of the University Health Network, Toronto, Ontario, Canada. SCI associated with arachnoiditis was induced as previously described [12]. Female Wistar rats approximately 250–300 g in weight were anesthetized with 2% isoflurane with oxygen and NO_2. The dorsal aspect of T6, T7 and T8 vertebra were removed and animals were subjected to a 35 g clip compression injury at T7 for 1 min followed by a subarachnoid injection of 0.5 mg/mL kaolin immediately rostral to the injury site. Multilayer tissue closure was then performed. Animals were anesthetized in the same fashion 24 h later, the injury site was reopened, animals were randomized and either 10 μL of HAMC or aCSF was injected intrathecally below the kaolin injection site.

2.3. Immunohistochemistry

Animals were fixed by transcardial perfusion with 4% paraformaldehyde (Sigma Aldrich, St Louis, MO, USA). Spinal cords were harvested and post-fixed in 4% paraformaldehyde containing 10% sucrose overnight followed by PBS containing 20% sucrose. Cords were then frozen in optimal cutting temperature (OCT) matrix and sectioned either transversely or longitudinally. Sections were rinsed in phosphate buffered saline (PBS) for 5 min and blocked in blocking solution (0.1% triton-X 100, 1% bovine serum albumin, 5% non fat milk, and 2.5% normal goat serum in PBS) for 1 h. Primary antibodies were incubated overnight in blocking solution minus triton-X 100 overnight at 4 °C (antibody solution). Primary antibodies included Iba-1 (Wako, Osaka, Japan), collagen IV (Abcam, Cambridge, MA, USA), GFAP (Millipore, Billerica, MA, USA), and CSPG (chondroitin sulfate proteoglycans; CS56 clone; Sigma). Sections were rinsed 3 × 10 min in PBS and fluorescent secondary antibodies [Alexa Flour 488 (green) and 568 (red); Invitrogen] were incubated for 2 h at room temperature in antibody solution. Sections were rinsed again in PBS and coverslipped in Mowoil mounting medium containing DAPI (Vector Laboratories, Burlingame, CA, USA). Cross section images include the distances from the injury epicenter and are shown with the dorsal aspect of the cord at the top of the image. In longitudinal sagittal sections, the images shown are taken from the spinal cord midline and are oriented with the dorsal aspect at the top and the rostral aspect at the left of the image.

2.4. Immunoblotting

All immunoblot reagents were purchased from Biorad (Hercules, CA, USA) unless otherwise stated. Animals were anesthetized and 0.5 cm of spinal cord tissue centered at the epicenter was removed and snap frozen in liquid nitrogen. The frozen tissue was crushed with a mortar and pestle in liquid nitrogen and added to a tube of ice-cold RIPA buffer (Thermo Scientific, Waltham, MA, USA). Equal protein amounts were determined using the Lowry method. For Western blots, homogenates were dissolved and boiled in sample buffer before PAGE on 12% gels and were then transferred to nitrocellulose membranes. For slot blot analysis, 3 μg of protein in RIPA buffer was blotted onto nitrocellulose membranes. Membranes were blocked with 5% nonfat milk in tris buffered saline with 0.05% tween-20 (TTBS) for 1 h at room temperature followed by the application of primary antibodies in blocking solution overnight at 4 °C. Membranes were then rinsed 3 × 10 min in TTBS and secondary horseradish peroxidase antibodies (Sigma) were incubated at room temperature for 1 h in blocking solution. Membranes were rinsed again in TTBS and enhanced chemiluminescence (ECL; Amersham) reagent and x-ray films were used to detect immunoreactivity. Average band densities were measured using a Flouro-S Imaging system and imaging software (Biorad). Primary antibodies included NF200 (Sigma), Iba-1 (Wako), GFAP and Actin (Millipore).

2.5. Multiplex ELISA

Tissue for multiplex ELISA was extracted and homogenized in ice-cold RIPA buffer (Thermo Scientific) and frozen. Samples were processed by Eve Technologies (Calgary, AB, Canada) using Rat Cytokine/Chemokine multiplex ELISA assays available from Millipore. Concentrations obtained from the assay were divided by protein concentration of the samples - determined by the Lowry method. Data are expressed as pg/mg protein.

2.6. Neurobehavioural assessments

All assessments were done with two blinded observers. Hindlimb locomotion was determined weekly for six weeks using the Basso Beattie Bresnahan (BBB) locomotor rating scale [22]. Motor function was determined biweekly using the inclined plane test [23]. Animals were placed horizontally on an inclined plane and the maximal angle they were able to maintain themselves on the plane for 5 s was recorded. At-level mechanical allodynia, a measure of neuropathic pain, was determined biweekly using 2 g and 4 g von Frey monofilaments as previously described [24]. Briefly, monofilaments were applied on the dorsal trunk around the injury site 10 times and adverse responses were recorded. An adverse response included vocalization, biting or licking, flinching or moving to the other end of the cage.

2.7. Electrophysiology

In vivo spinal cord evoked potentials (SCEP) were recorded from rats at 6 weeks following injury. These electrophysiological outcome measures have been used widely in our laboratory [25,26]. The spinal cord at T8-9 was stimulated (2 mA; 0.13 Hz; 0.04 ms) and responses were recorded from the spinal cord at C2-3 (20 sweeps). A bandpass filter of 10–3000 Hz was used. Amplitude was measured from the first major positive peak to the first major negative peak. Response latency was determined by measuring the time between the appearance of the stimulus artifact and the first positive peak. Conduction velocity was calculated from SCEP recordings by dividing the distance between the stimulating and recording electrodes by the latency.

2.8. Magnetic resonance imaging (MRI)

MR imaging was carried out at the STTARR facility in Toronto, Ontario using a Buker Biospec Scanner and 7T magnet. T2 Turbo RARE (Rapid Acquisition Relaxation Enhanced) - aka Fast Spin Echo (FSE) sequences were run with the following parameters: TE = 8.856 ms, Effective TE = 43.28 ms, TR = 1500 ms, RareFactor = 16, NEX (number of excitations = # of averages) = 3, Scan time = 21m36s. Voxel information collected was as follows: 50 × 50 × 16 mm (FOV), 250 × 150 × 32 (matrix) and 200 × 333 × 500 um (voxel size/resolution). Respiratory gating was used during imaging. Lesion volumes were calculated by a blinded observer using Matlab ® software by measuring the region of hyperintense voxels in each slice and summing the value from each slice in an animal.

2.9. Data presentation and statistics

All error bars represent standard error of the mean (SEM). Statistics were done using StatPlus:mac Version 2009 software (AnalystSoft Inc., Alexandria, VA, USA). Behavioural data were analyzed by two way analysis of variance (ANOVA) tests with Bonferroni post-hoc tests. Densitometry and SCEPs were analyzed with *t*-tests. In light of the fact that the neuropathic pain, cytokine and immunohistochemical lesion size analyses exhibited skewed, non-normal distributions, logarithmic transformations were applied prior to statistical analysis. Subsequently, cytokine outcomes were compared between the treatment groups using a two way ANOVA technique to adjust for slight variations in experimental conditions depending on the cohort of animals examined. The number of animals per group is included in the results section and figure legends. In certain cases, comparisons between treatment and control groups failed to reach significance, however, fell within one alpha level of significance (ie. $p < 0.1$). These data, while not significant at 95% confidence, were described as exhibiting a trend.

3. Results

3.1. Meningeal inflammation and fibrosis

HAMC or aCSF control was injected intrathecally caudal to the kaolin injury site/area of scarring 24 h following injury. The spread of subarachnoid inflammation and scarring was examined 7 days post injury. Since kaolin remains present in the subarachnoid space after injection, we sought to qualitatively observe the caudal spread of the inflammation and scarring that its presence caused through immunohistochemistry. Interestingly, HAMC attenuated the longitudinal extent of arachnoiditis and meningeal fibrosis, as shown in Fig. 1. Fig. 1A shows representative sagittal sections stained for collagen-IV (red) and CSPGs (green) in aCSF and HAMC treated animals. With HAMC treatment, the spread of scarring caudally from the site of kaolin injection (boxed area) was significantly reduced. Similarly, Iba-1 (green) staining demonstrated that HAMC reduced the extent of macrophage/microglia in the meninges 7 days post injury compared to aCSF controls (Fig. 1B).

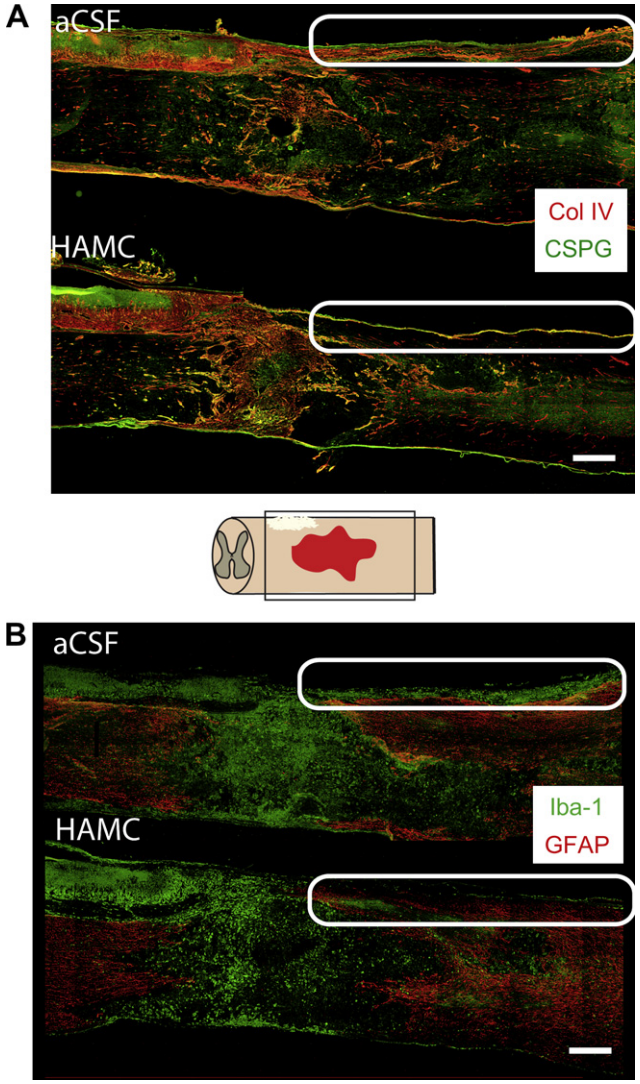

Fig. 1. HAMC reduces the caudal spread of induced arachnoiditis and meningeal fibrosis. (A) Immunofluorescence images show collagen-IV (red) and CSPG (green) expression in aCSF and HAMC treated animals, 7 days following injury. In HAMC treated animals, the extent of scarring spreading caudal from the site of kaolin injection (boxed area) is markedly reduced. (B) Iba-1 (green) staining demonstrates that HAMC also reduced the caudal presence of macrophage/microglia in the meninges at 7 days post injury. GFAP is shown in red. In both parts, images are taken from the sagittal midline of the spinal cord. Scale bar represents 1 mm. The central diagram shows the orientation of the images. (For interpretation of the references to colour in this figure legend, the reader is referred to the web version of this article.)

3.2. Neurobehavioural outcomes

Animals were monitored weekly for hindlimb locomotor activity in an open field, according to the BBB locomotor rating scale. Fig. 2A shows that HAMC injection significantly improved the locomotor recovery compared to aCSF controls (two way ANOVA $p < 0.05$, $n = 12$ per group). The effect was seen most robustly at 6 weeks, where there was an increase of 1.6 points in HAMC treated animals (Bonferroni post-hoc test, $p < 0.05$). In addition to weekly locomotor assessments, motor function was monitored biweekly using the inclined plane apparatus. Fig. 2B demonstrates that HAMC did not improve function on the inclined plane relative to aCSF controls (two way ANOVA, $p = 0.88$; $n = 12$ per group).

In vivo spinal cord evoked potentials (SCEPs) were recorded from rats 6 weeks following injury ($n = 4$ per group). The average conduction velocities and amplitudes are shown in Fig. 2C. HAMC treated animals exhibited a significant increase in average conduction velocity compared to aCSF controls (*t*-test, $p < 0.05$). Similarly, HAMC animals exhibited a significant increase in the average amplitude compared to aCSF controls (*t*-test, $p < 0.05$). Representative traces are shown below the graphs.

At 4 and 6 weeks following injury, treated and control animals were also monitored for the incidence of at-level mechanical allodynia, a measure of neuropathic pain. Application of von Frey monofilaments (2 g or 4 g) was carried out on the dorsal aspect of the rats around the level of injury for a total of 10 times. The average number of adverse reactions in aCSF and HAMC treated animals is shown Fig. 2C ($n = 12$ animals per group). There was an overall treatment effect with HAMC using the 2 g monofilament (ANOVA, $p < 0.05$). However, group comparisons revealed non-significant decreases at 4 weeks and 6 weeks (Bonferroni post-hoc test, $p = 0.23$ and $p = 0.1$, for 4 and 6 weeks, respectively). There was no difference between aCSF and HAMC treated animals when using the 4 g monofilament (two way ANOVA, $p = 0.24$).

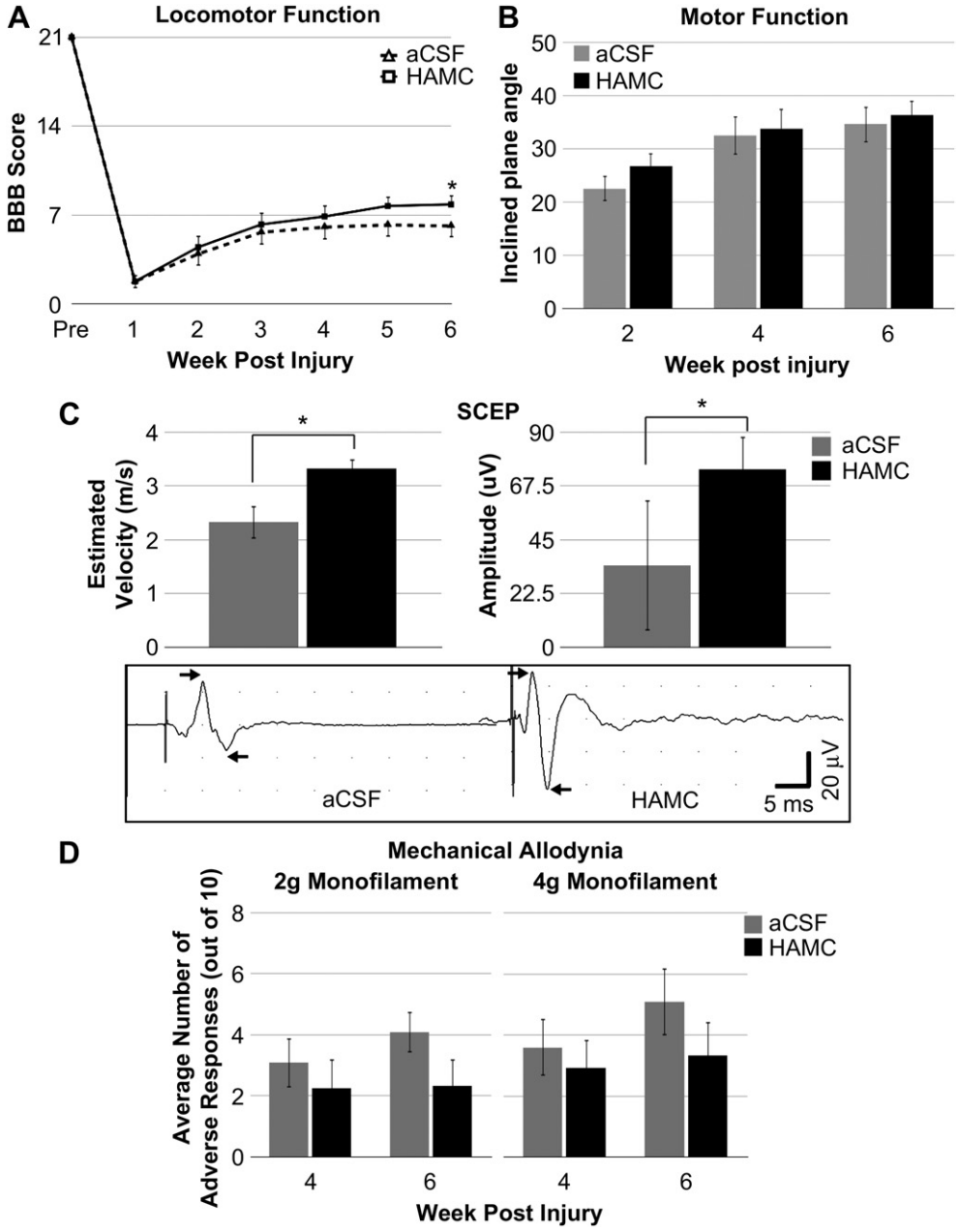

Fig. 2. HAMC improves neurobehavioural outcome. (A) HAMC injection significantly improved the locomotor recovery compared to aCSF controls according to the BBB locomotor rating scale (two way ANOVA $p < 0.05$; $n = 12$ per group). At week 6, there was a 1.6-point difference between aCSF and HAMC treated animals (* Bonferroni post-hoc test, $p < 0.05$). (B) HAMC did not improve motor function compared to aCSF controls as assessed by the inclined plane apparatus (two way ANOVA, $p = 0.88$; $n = 12$ per group). (C) *In vivo* SCEP were recorded from rats 6 weeks following injury. HAMC animals exhibited a significant increase in conduction velocity and amplitude compared to aCSF animals. ($n = 4$ per group; *t-test, $p < 0.05$ for each). Representative traces are shown. (D) The incidence of at level mechanical allodynia, a measure of neuropathic pain, was monitored with von Frey monofilaments (2 g or 4 g). The average number of adverse responses to 10 applications of the monofilament is shown ($n = 12$). There was an overall treatment effect with HAMC when using the 2 g monofilament (two way ANOVA, $p < 0.05$), however, group comparisons were not found to be statistically significant (Bonferroni post-hoc test, $p = 0.23$ for week 4 and $p = 0.1$ for week 6). Using the 4 g monofilament, there was no difference between aCSF and HAMC treated animals (two way ANOVA, $p = 0.24$). Error bars represent SEM.

3.3. Lesion size analysis

Following the 6 week behavioural analysis, animals were subjected to MR imaging to determine spinal cord lesion size. Longitudinal T2-weighted images were produced using the parameters described in the methods section, with each image corresponding to an approximate 500 μm thick sagittal section. Fig. 3A shows a representative slice through the midline of the spinal cord in an aCSF control and HAMC treated animal. Hyperintense voxels in each image slice were traced using Matlab® software and summed, generating an approximate lesion volume for each animal. The average lesion volume from each group is reported in Fig. 3A ($n = 12$ per group). HAMC treatment led to a non-significant decrease in lesion volume compared to aCSF controls (23% decrease; t-test, $p = 0.11$).

Following MR imaging, animals were perfused with PFA and 20 μm thick frozen sagittal sections were generated. Sections were processed for GFAP immunoreactivity to delineate the lesion boundaries. Representative sagittal GFAP images for aCSF and HAMC animals are shown in Fig. 3B. The lesion area was measured in 5 sections per animal, spaced 500 μm apart using ImageJ® software. Average lesion area for each group is demonstrated.

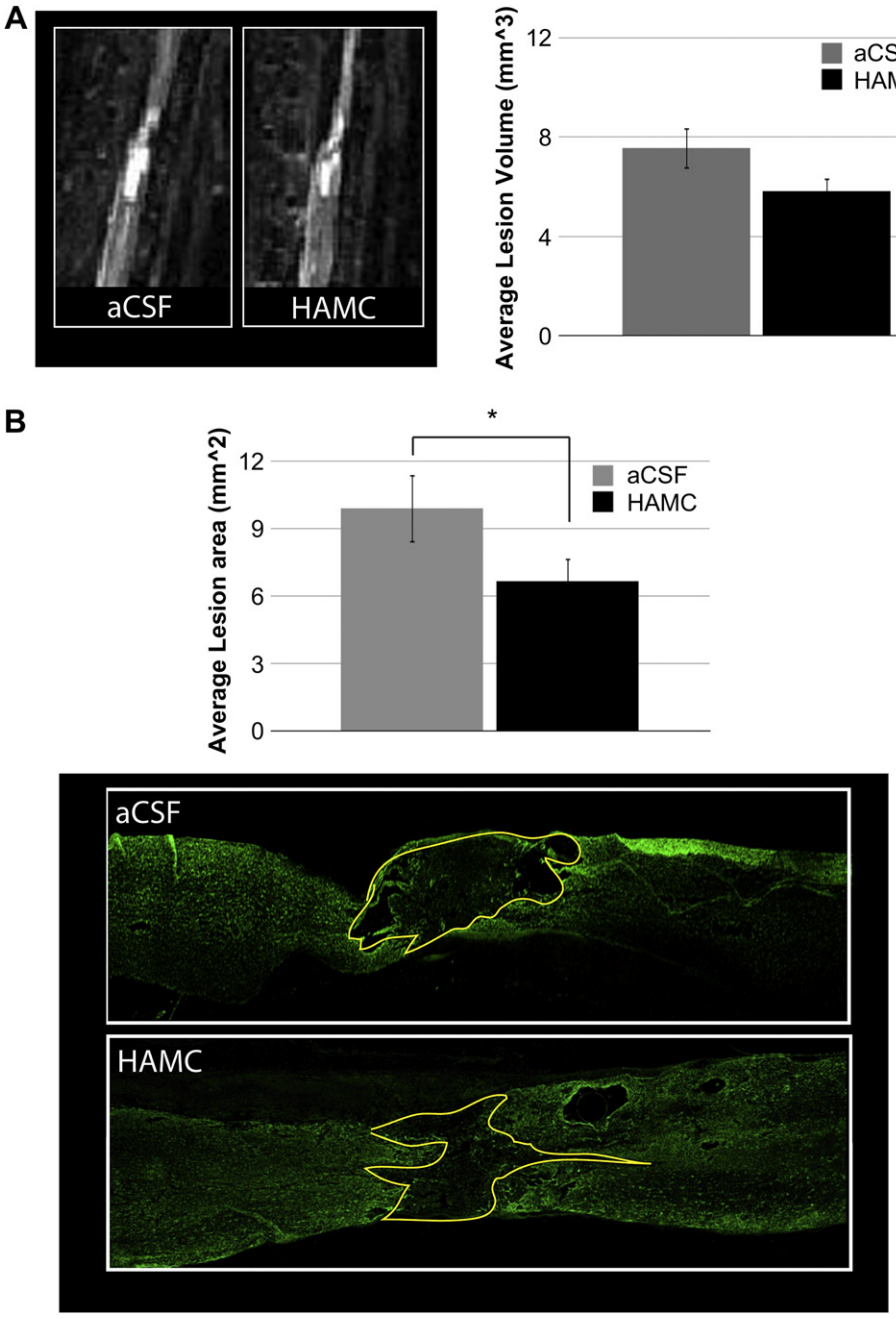

Fig. 3. HAMC reduces lesion size. (A) Longitudinal T2-weighted MR images were taken 6 weeks following injury. Representative slices through the midline of the spinal cord in an aCSF control and HAMC treated animal are shown. HAMC reduced the lesion volume compared to aCSF animals, however the extent was not found to be significant ($n = 12$ per group; t-test, $p = 0.11$). (B) Following MR imaging, GFAP immunofluorescence was used to delineate the lesion borders and average lesion areas were calculated. Representative images from aCSF and HAMC animals are shown. HAMC treatment reduced the lesion area by approximately 32% ($n = 8$ per group; *t-test $p < 0.05$). Error bars represent SEM.

HAMC treatment significantly reduced the lesion area compared to aCSF controls (32% decrease; t-test, $p < 0.05$).

3.4. Cellular inflammation and axonal preservation

To support behavioural and histological analyses, we determined the effect of HAMC on inflammatory cell activation and axonal preservation following injury. We looked at MPO activity at 2 days post injury as a measure of neutrophil extravasation and Iba-1 protein expression at 7 days post injury as a semi-quantitative measure of macrophage and microglia ($n = 6$ per group). Fig. 4A demonstrates that HAMC did not reduce MPO activity compared to aCSF controls in either granular or cytoplasmic/ECM homogenate fractions (t-test, $p = 0.6$ and $p = 0.2$, respectively). Fig. 4B demonstrates Western blot analysis of Iba-1 protein expression 7 days following injury. There was no difference in the relative densities between aCSF and HAMC animals ($n = 6$ per group; $p = 0.88$). Representative Iba-1 Western blot bands are shown for non-injured controls (sham), aCSF and HAMC animals.

We also assessed axonal preservation 2 days following injury through NF200 expression. Fig. 4C shows representative Western blot bands for non-injured controls (sham), aCSF and HAMC animals in addition to semi-quantitative densitometry results ($n = 12$ per group). HAMC treatment showed a trend towards

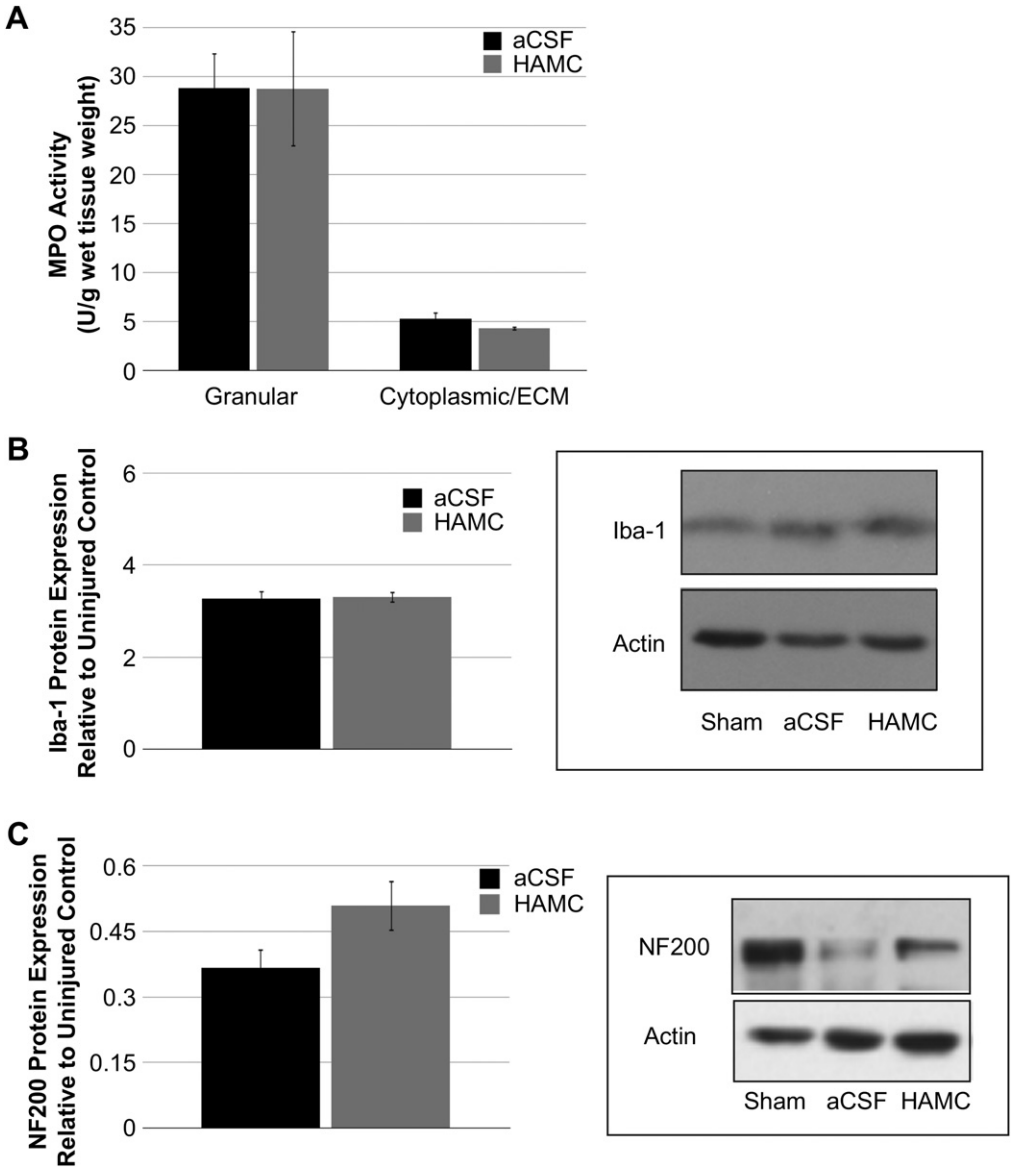

Fig. 4. HAMC does not reduce neutrophil or macrophage/microglial activation but does show a trend towards axonal preservation. (A) Granular and cytoplasmic/ECM fractions were assessed for MPO activity as a measure of neutrophil activation, 2 days following injury. HAMC did not alter MPO activity in either fraction compared to aCSF controls ($n = 6$ per group; t-test, $p = 0.6$ $p = 0.23$, respectively). (B) Microglial/macrophage activation was determined with Iba-1 expression at 7 days post injury with Western blotting. There was no difference in Iba-1 protein expression between aCSF and HAMC treated animals ($n = 6$ per group; t-test, $p = 0.88$). (C) At 2 days post injury, axonal preservation was assessed with Western blotting for NF200 expression. HAMC showed a trend towards increased NF200 expression compared to aCSF controls ($n = 12$ per group; t-test, $p = 0.06$). Error bars represent SEM.

increased NF200 expression compared to aCSF controls (t-test, $p = 0.063$).

3.5. Fibrous and glial scarring

Next, we assessed fibrous and glial scarring by looking at the expression of CSPGs and GFAP, respectively at 7 days post injury. Fig. 5A demonstrates representative slot blot bands for non-injured control (sham), aCSF and HAMC animals along with semi-quantitative densitometry for CSPGs ($n = 6$ per group). HAMC significantly decreased CSPG expression compared to aCSF controls (t-test, $p < 0.01$). Representative slot blot and semi-quantitative densitometry for GFAP is shown in Fig. 5B ($n = 6$ per group). GFAP immunoreactivity was not found to be different between aCSF and HAMC treated animals (t-test, $p = 0.43$). Immunohistochemistry for CSPGs (red) and GFAP (green) is shown in Fig. 5C. Fluorescent images were taken from transverse sections located at 2000 μm rostral and caudal from the injury epicenter. These images demonstrate that there is less parenchymal CSPG deposition in HAMC treated animals.

3.6. Inflammatory cytokine and chemokine expression

To gain greater insight into the mechanism by which HAMC may be acting, we examined differences in cytokine and chemokine expression after HAMC injection, 2 days following injury (or 1 day after HAMC injection). Fig. 6A shows average cytokine levels and Fig. 6B shows average chemokine levels. Data are presented as pg/mg protein ($n = 12$ per group). HAMC reduced IL-1α expression (two way ANOVA, $p < 0.05$) but did not significantly reduce IL-6 ($p = 0.12$), IL-1β ($p = 0.28$) or TNF-α ($p = 0.74$). Additionally, HAMC did not significantly reduce MCP-1 ($p = 0.33$), GRO/KC

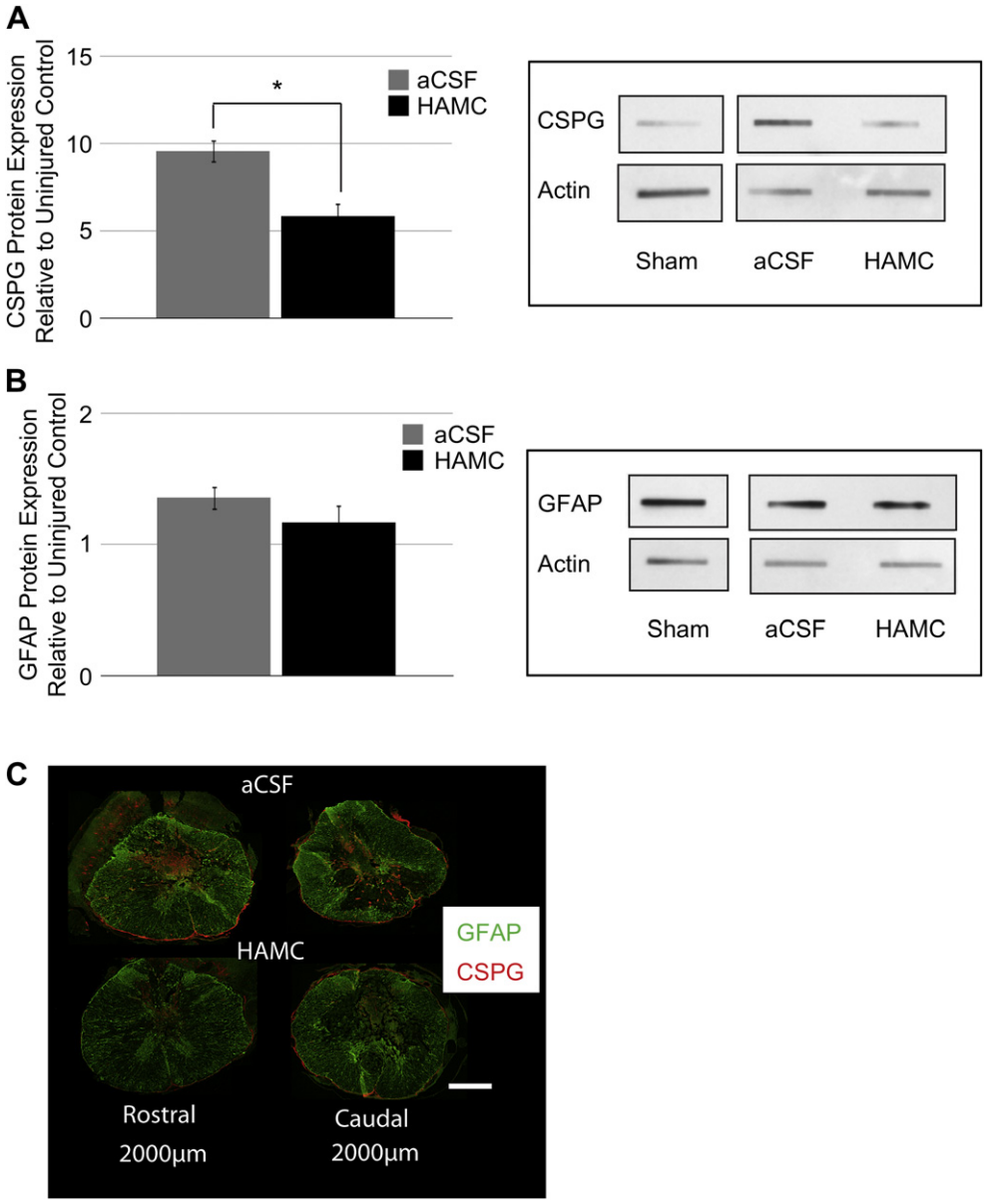

Fig. 5. HAMC reduces CSPG expression. Slot blotting was used to determine (A) CSPG and (B) GFAP expression 7 days following injury. Representative bands from non-injured control animals (sham), aCSF and HAMC animals are shown. (A) HAMC treatment reduced CSPG expression relative to aCSF controls (*t-test, $p < 0.01$). (B) HAMC treatment did not alter GFAP expression relative to aCSF controls (t-test, $p = 0.43$). (C) Transverse immunofluorescence images show GFAP (green) and CSPG (red) expression 7 days following injury at 2000 μm rostral and caudal from the injury epicenter. Note the reduced CSPG expression in the parenchyma of HAMC treatment animals. Scale bar represents 1 mm. Error bars represent SEM ($n = 6$ per group).

($p = 0.55$) or MIP-1α ($p = 0.11$) expression compared to aCSF controls.

4. Discussion

We have demonstrated that injection of a hydrogel containing HA improved neurobehavioural recovery and histological outcome following SCI associated with subarachnoid scarring. The physical blend of HAMC reduced the extent of scarring and inflammation in the subarachnoid space. While there was no overall reduction in macrophage/microglia or neutrophils following injury, HAMC showed a trend towards axonal preservation and a significant reduction in both IL-1α and CSPG expression following injury.

While others have used urokinase to reduce fibrosis in models of arachnoiditis (not associated with SCI) [27], to our knowledge this is one of the first studies to look directly at reducing subarachnoid scarring following traumatic injury to the spinal cord. Some groups have suggested that HA can modulate inflammatory reactions [20], fibrous scarring and improve functional recovery following SCI [18,28]. In our HAMC, HA is likely the putative therapeutic molecule, and not MC, based on *in vitro* studies in microglia (paper in preparation).

Following SCI, endogenous HA (10^6 Da) is degraded [29] – possibly by endogenous hyaluronidases (see [30] for a review) and reactive oxygen species [31]. While the anti-inflammatory benefits of exogenous HMW-HA (above 1000 kDa) have been demonstrated [32,33], there is evidence that HA of lower molecular weights (LMW-HA) can be pro-inflammatory [34]. However, studies have also shown that LMW-HA can also be anti-inflammatory [35] and pro-angiogenic [36]. Moreover, delivery of HA oligomers (from 2 to 12 saccharides; corresponding to 372–2233 g/mol) to the injured spinal cord showed improved functional recovery in a weight drop

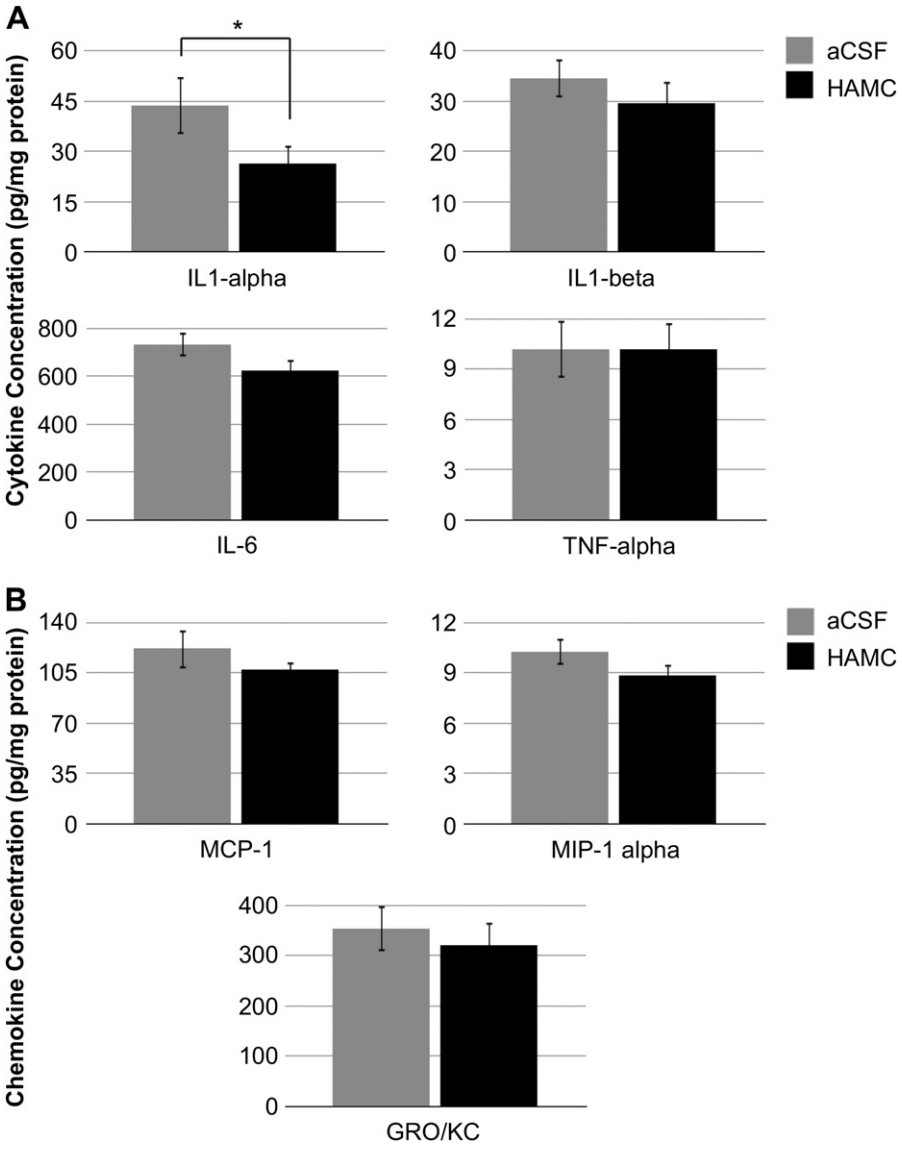

Fig. 6. HAMC reduces IL-1α cytokine expression. Cytokine and chemokine expression was determined by multiplex ELISA from tissue isolated 2 days following injury. (A) HAMC reduced IL-1α (two way ANOVA, $p < 0.05$) but did not significantly alter the expression of IL-1β ($p = 0.28$), IL-6 ($p = 0.12$) or TNF-α ($p = 0.74$) compared to aCSF controls. (B) HAMC did not significantly reduce MCP-1 ($p = 0.33$), GRO/KC ($p = 0.55$) or MIP-1α ($p = 0.11$) protein levels relative to aCSF controls. Error bars represent SEM. ($n = 12$ per group).

model of SCI in rats [28]. Together, it is expected that the molecular state of exogenous HA in regards to the pathophysiology of SCI is complex and could influence inflammation, fibrous scarring and angiogenesis at various stages of biodegradation.

The treatment effects of HAMC can be described in terms of its influence on meninges and parenchyma. The injection of HAMC into the subarachnoid space puts it into contact with inflammatory cells and local meningeal fibroblasts activated from SCI and induced arachnoiditis. The physical presence of HAMC and/or chemical interactions of free HA released into the CSF upon biodegradation may have acted in tandem to influence the number of inflammatory cells recruited to the meninges (as in Fig. 1), the inflammatory mediators produced by these cells and from meningeal fibroblasts. As there is significant exchange of extracellular fluid and CSF (see [37] for a review of CSF pathways), reduced meningeal inflammation is expected to influence cells in the parenchyma. Evidence that parenchymal pathophysiological was altered is demonstrated by a reduced lesion size (Fig. 3), CSPG expression (Fig. 5) and a trend towards axonal preservation (Fig. 4).

HAMC showed a modest improvement in hindlimb locomotion following SCI compared to aCSF controls (Fig. 2A). This was supported by a trend towards axonal preservation through NF200 immunoblotting at 2 days following injury (Fig. 4C) and improved SCEP axonal conduction (Fig. 2C), though this measured afferent cord conduction. In contrast, motor function was not improved as measured by the inclined plane test (Fig. 2B). This discrepancy could be explained by the fact that the inclined plane test was developed using a cervical injury (C7-T1) [23,38] whereas the BBB was developed using thoracic injuries [22]. Thus, the inclined plane test, while still useful, is likely not as sensitive for thoracic injuries as the BBB in terms of measuring small changes in functional improvement.

We also observed that there was an overall treatment effect on at-level mechanical allodynia (Fig. 2D). However, this treatment effect was not found to be significant at 4 and 6 weeks post injury when post-hoc tests were performed. Interestingly, only half of the untreated animals developed mechanical allodynia in our model, which is similar to what others have observed in different models

of neuropathic pain [39], yet which also limited our power to determine treatment effect. Similar to our PTS model, not all cases of human SCI develop neuropathic pain [40,41]. It should be noted that survival of dorsal horn neurons caudal to the injury site (data not shown) and SCEP recordings (Fig. 2C) suggest there was not a bias in pain relaying infrastructure that could account for any differences in pain response between HAMC and aCSF animals.

Previous studies from other groups suggest that HA reduces microglia/macrophage activation following SCI [18,28]. However, using Western blotting, our study did not detect a reduction in microglia/macrophage activation (Fig. 4B). The source and size of HA, delivery methods and injury models were different from our study and could explain the different results. In terms of microglia/macrophage activation, our study also looked at Iba-1, OX42 (CD11b) and ED-1 (CD68) gene expression using qPCR and found no treatment differences (data not shown). Additionally, we carried out immunoblotting and qPCR analyses at 2 and 7 days post injury and in tissue adjacent to the injury epicenter (0.5 cm rostral and caudal) and found no treatment differences (data not shown). It is possible, however, that small spatial decreases in macrophage/microglia, that are detectable with immunohistochemistry, are lost when a larger section of homogenized tissue is analyzed.

Our study showed a reduction in CSPG expression (Fig. 5), which is consistent with previous studies [18,28]. Importantly, through immunohistochemistry we demonstrated that CSPGs were reduced in the parenchyma of HAMC treated animals (Fig. 5C), suggesting that the reduction seen in CSPG expression from homogenate samples in Fig. 5 was not solely due to less CSPGs in the meninges as shown in Fig. 1. As HAMC was found to influence fibrous scarring, it might have been able to promote endogenous regeneration due to decreased CSPG expression. Indeed, studies that have reduced CSPG expression following injury through enzymatic degradation have led to enhanced endogenous regeneration and plasticity [42,43]; however, we recognize that some of the effects in these studies could be attributable to other mechanisms [44].

We were able to detect a significant decrease in IL-1α expression in HAMC treated animals compared to aCSF controls. Additionally, we saw non-significant decreases in IL-6 and MIP-1α. Together, this reflects the possibility of a very modest reduction of inflammatory cytokine/chemokine expression. The link with inflammatory cytokines/chemokines and neurotoxicity in addition to preventing axonal growth is well established in the literature [45,46], thus the decreases, though not all statistically significant, may have had a biological effect on injury pathophysiology. Related to this, we observed a trend in axonal preservation (Fig. 4) that could be due to less cytokine/chemokine production. Due to the lack of statistical significance, this proposed relationship is only speculative.

It is interesting to think about whether we could translate this strategy to the clinic. We have demonstrated that administration of HAMC is beneficial following SCI associated with arachnoiditis based on acute application of the therapeutic. While PTS is considered a chronic complication of SCI, studies have described cases developing within several weeks to months following SCI [9,47,48]. Furthermore, it is possible that acute to sub-acute arachnoiditis – which we are targeting in this study – is the cause of the chronic subarachnoid scarring associated with PTS.

This study has implications not only for SCI but also for other CNS conditions. Any time the dura is breached, the risk of causing local inflammation and subarachnoid scarring exist. Certain situations lend themselves to the application of a biodegradable, non-cell adhesive, anti-inflammatory compound that could offer a prolonged effect until the inflammatory response has subsided. These include subdural surgical procedures such as tumor removal, stem cell injections, surgery for a subdural/subarachnoid hemorrhage and decompressive/arachnolysis treatment for PTS. In particular, the surgical procedures of shunting and arachnolysis for chronic PTS are prone to failure, including a high recurrence of meningeal scarring/fibrosis [1,49] and return of the syrinx. Overall, we feel that an anti-inflammatory hydrogel like HAMC could be suitable as an adjuvant therapy to subdural surgical procedures.

5. Conclusions

In summary, HAMC dampened arachnoiditis associated with SCI and improved functional recovery. In addition to improving neurobehavioural and neuroanatomical outcomes, HAMC reduced IL-1α cytokine expression and CSPG expression. These findings should be of interest to the PTS community, who currently are without effective treatment options. Furthermore, HAMC represents a possible strategy for surgeons to mitigate arachnoid inflammation and scarring related to subdural surgical procedures. Though its effects were modest in our model, future studies elucidating the efficacy of HAMC are certainly warranted. HAMC could be further tested pre-clinically in the context of preventing arachnoid scarring and adhesions from returning following surgical procedures for detethering/dissection of the arachnoid scar. Additionally, HAMC could be used as a drug delivery vehicle (as it was originally developed) to further reduce the inflammatory response and scarring in the subarachnoid space in models of PTS.

Acknowledgements

The authors would like to acknowledge Behzad Azad for help with the neurobehavioural analysis and Warren Foltz at the STTARR facility for assistance with MR imaging. This work was supported by a grant from the Physicians Services Incorporated, the Canadian Syringomyelia Network and the Krembil Chair in Neural Repair and Regeneration (MGF). We are grateful for partial financial support from the McLaughlin Center for Molecular Medicine and the McEwen Center for Regenerative Medicine. JWA was supported by the CIHR Vanier Doctoral Award and an Ontario Graduate Scholarship. CEK was supported by funding from the Ontario Neurotrauma Foundation and Canadian Institutes of Health Research (CIHR, to MSS). MDB was supported by an NSERC Doctoral Canada Graduate Scholarship.

References

[1] Klekamp J, Batzdorf U, Samii M, Bothe HW. Treatment of syringomyelia associated with arachnoid scarring caused by arachnoiditis or trauma. J Neurosurg 1997;86:233–40.
[2] Backe HA, Betz RR, Mesgarzadeh M, Beck T, Clancy M. Post-traumatic spinal cord cysts evaluated by magnetic resonance imaging. Paraplegia 1991;29:607–12.
[3] Williams B. Pathogenesis of post-traumatic syringomyelia. Br J Neurosurg 1992;6:517–20.
[4] Wang D, Bodley R, Sett P, Gardner B, Frankel H. A clinical magnetic resonance imaging study of the traumatised spinal cord more than 20 years following injury. Paraplegia 1996;34:65–81.
[5] Perrouin-Verbe B, Lenne-Aurier K, Robert R, Auffray-Calvier E, Richard I, Mauduyt de la Greve I, et al. Post-traumatic syringomyelia and post-traumatic spinal canal stenosis: a direct relationship: review of 75 patients with a spinal cord injury. Spinal Cord 1998;36:137–43.
[6] Abel R, Gerner HJ, Smit C, Meiners T. Residual deformity of the spinal canal in patients with traumatic paraplegia and secondary changes of the spinal cord. Spinal Cord 1999;37:14–9.
[7] Stoodley MA. Pathophysiology of syringomyelia. J Neurosurg 2000;92:1069–70. author reply 71–3.
[8] Schwartz ED, Falcone SF, Quencer RM, Green BA. Posttraumatic syringomyelia: pathogenesis, imaging, and treatment. AJR Am J Roentgenol 1999;173:487–92.
[9] Vannemreddy SS, Rowed DW, Bharatwal N. Posttraumatic syringomyelia: predisposing factors. Br J Neurosurg 2002;16:276–83.
[10] Todor DR, Mu HT, Milhorat TH. Pain and syringomyelia: a review. Neurosurg Focus 2000;8:E11.

[11] Brodbelt AR, Stoodley MA. Post-traumatic syringomyelia: a review. J Clin Neurosci 2003;10:401–8.
[12] Seki T, Fehlings MG. Mechanistic insights into posttraumatic syringomyelia based on a novel in vivo animal model. Laboratory investigation. J Neurosurg Spine 2008;8:365–75.
[13] Sakiyama-Elbert SE, Hubbell JA. Development of fibrin derivatives for controlled release of heparin-binding growth factors. J Control Release 2000; 65:389–402.
[14] Laverty PH, Leskovar A, Breur GJ, Coates JR, Bergman RL, Widmer WR, et al. A preliminary study of intravenous surfactants in paraplegic dogs: polymer therapy in canine clinical SCI. J Neurotrauma 2004;21:1767–77.
[15] Luo J, Borgens R, Shi R. Polyethylene glycol immediately repairs neuronal membranes and inhibits free radical production after acute spinal cord injury. J Neurochem 2002;83:471–80.
[16] Kim H, Zahir T, Tator CH, Shoichet MS. Effects of dibutyryl cyclic-AMP on survival and neuronal differentiation of neural stem/progenitor cells transplanted into spinal cord injured rats. PLoS One 2011;6:e21744.
[17] Hejcl A, Lesny P, Pradny M, Sedy J, Zamecnik J, Jendelova P, et al. Macroporous hydrogels based on 2-hydroxyethyl methacrylate. Part 6: 3D hydrogels with positive and negative surface charges and polyelectrolyte complexes in spinal cord injury repair. J Mater Sci Mater Med 2009;20:1571–7.
[18] Khaing ZZ, Milman BD, Vanscoy JE, Seidlits SK, Grill RJ, Schmidt CE. High molecular weight hyaluronic acid limits astrocyte activation and scar formation after spinal cord injury. J Neural Eng 2011;8:046033.
[19] Jiang D, Liang J, Noble PW. Hyaluronan in tissue injury and repair. Annu Rev Cell Dev Biol 2007;23:435–61.
[20] Gupta D, Tator CH, Shoichet MS. Fast-gelling injectable blend of hyaluronan and methylcellulose for intrathecal, localized delivery to the injured spinal cord. Biomaterials 2006;27:2370–9.
[21] Kang CE, Poon PC, Tator CH, Shoichet MS. A new paradigm for local and sustained release of therapeutic molecules to the injured spinal cord for neuroprotection and tissue repair. Tissue Eng Part A 2009;15:595–604.
[22] Basso DM, Beattie MS, Bresnahan JC. A sensitive and reliable locomotor rating scale for open field testing in rats. J Neurotrauma 1995;12:1–21.
[23] Rivlin AS, Tator CH. Objective clinical assessment of motor function after experimental spinal cord injury in the rat. J Neurosurg 1977;47:577–81.
[24] Bruce JC, Oatway MA, Weaver LC. Chronic pain after clip-compression injury of the rat spinal cord. Exp Neurol 2002;178:33–48.
[25] Fehlings MG, Tator CH, Linden RD, Piper IR. Motor and somatosensory evoked potentials recorded from the rat. Electroencephalogr Clin Neurophysiol 1988; 69:65–78.
[26] Nashmi R, Fehlings MG. Changes in axonal physiology and morphology after chronic compressive injury of the rat thoracic spinal cord. Neuroscience 2001; 104:235–51.
[27] Ceviz A, Arslan A, Ak HE, Inaloz S. The effect of urokinase in preventing the formation of epidural fibrosis and/or leptomeningeal arachnoiditis. Surg Neurol 1997;47:124–7.
[28] Wakao N, Imagama S, Zhang H, Tauchi R, Muramoto A, Natori T, et al. Hyaluronan oligosaccharides promote functional recovery after spinal cord injury in rats. Neurosci Lett 2011;488:299–304.
[29] Struve J, Maher PC, Li YQ, Kinney S, Fehlings MG, Kuntz Ct, et al. Disruption of the hyaluronan-based extracellular matrix in spinal cord promotes astrocyte proliferation. Glia 2005;52:16–24.
[30] Jiang D, Liang J, Noble PW. Hyaluronan as an immune regulator in human diseases. Physiol Rev 2011;91:221–64.
[31] Bates EJ, Harper GS, Lowther DA, Preston BN. Effect of oxygen-derived reactive species on cartilage proteoglycan-hyaluronate aggregates. Biochem Int 1984; 8:629–37.
[32] Yasuda T. Hyaluronan inhibits prostaglandin E2 production via CD44 in U937 human macrophages. Tohoku J Exp Med 2010;220:229–35.
[33] Yasuda T. Hyaluronan inhibits cytokine production by lipopolysaccharide-stimulated U937 macrophages through down-regulation of NF-kappaB via ICAM-1. Inflamm Res 2007;56:246–53.
[34] Taylor KR, Yamasaki K, Radek KA, Di Nardo A, Goodarzi H, Golenbock D, et al. Recognition of hyaluronan released in sterile injury involves a unique receptor complex dependent on Toll-like receptor 4, CD44, and MD-2. J Biol Chem 2007;282:18265–75.
[35] Kawana H, Karaki H, Higashi M, Miyazaki M, Hilberg F, Kitagawa M, et al. CD44 suppresses TLR-mediated inflammation. J Immunol 2008;180:4235–45.
[36] Slevin M, Krupinski J, Gaffney J, Matou S, West D, Delisser H, et al. Hyaluronan-mediated angiogenesis in vascular disease: uncovering RHAMM and CD44 receptor signaling pathways. Matrix Biol 2007;26:58–68.
[37] Brodbelt A, Stoodley M. CSF pathways: a review. Br J Neurosurg 2007;21: 510–20.
[38] Midha R, Fehlings MG, Tator CH, Saint-Cyr JA, Guha A. Assessment of spinal cord injury by counting corticospinal and rubrospinal neurons. Brain Res 1987;410:299–308.
[39] Nesic O, Lee J, Johnson KM, Ye Z, Xu GY, Unabia GC, et al. Transcriptional profiling of spinal cord injury-induced central neuropathic pain. J Neurochem 2005;95:998–1014.
[40] Finnerup NB, Johannesen IL, Sindrup SH, Bach FW, Jensen TS. Pain and dysesthesia in patients with spinal cord injury: a postal survey. Spinal Cord 2001; 39:256–62.
[41] Siddall PJ, McClelland JM, Rutkowski SB, Cousins MJ. A longitudinal study of the prevalence and characteristics of pain in the first 5 years following spinal cord injury. Pain 2003;103:249–57.
[42] Bradbury EJ, Moon LD, Popat RJ, King VR, Bennett GS, Patel PN, et al. Chondroitinase ABC promotes functional recovery after spinal cord injury. Nature 2002;416:636–40.
[43] Barritt AW, Davies M, Marchand F, Hartley R, Grist J, Yip P, et al. Chondroitinase ABC promotes sprouting of intact and injured spinal systems after spinal cord injury. J Neurosci 2006;26:10856–67.
[44] Carter LM, Starkey ML, Akrimi SF, Davies M, McMahon SB, Bradbury EJ. The yellow fluorescent protein (YFP-H) mouse reveals neuroprotection as a novel mechanism underlying chondroitinase ABC-mediated repair after spinal cord injury. J Neurosci 2008;28:14107–20.
[45] Lacroix S, Chang L, Rose-John S, Tuszynski MH. Delivery of hyper-interleukin-6 to the injured spinal cord increases neutrophil and macrophage infiltration and inhibits axonal growth. J Comp Neurol 2002;454:213–28.
[46] Perrin FE, Lacroix S, Aviles-Trigueros M, David S. Involvement of monocyte chemoattractant protein-1, macrophage inflammatory protein-1alpha and interleukin-1beta in Wallerian degeneration. Brain 2005;128:854–66.
[47] Sgouros S, Sharif S. Post-traumatic syringomyelia producing paraplegia in an infant. Childs Nerv Syst 2008;24:357–60. discussion 61–4.
[48] Carroll AM, Brackenridge P. Post-traumatic syringomyelia: a review of the cases presenting in a regional spinal injuries unit in the north east of England over a 5-year period. Spine (Phila Pa 1976) 2005;30:1206–10.
[49] Wiart L, Dautheribes M, Pointillart V, Gaujard E, Petit H, Barat M. Mean term follow-up of a series of post-traumatic syringomyelia patients after syringo-peritoneal shunting. Paraplegia 1995;33:241–5.